Received June 21, 2020, accepted June 27, 2020, date of publication July 14, 2020, date of current version August 4, 2020.

Digital Object Identifier 10.1109/ACCESS.2020.3009188

Robust Extended H_∞ Control Strategy Using Linear Matrix Inequality Approach for Islanded Microgrid

MANIZA ARMIN[1], MIZANUR RAHMAN[1], MD. MUKIDUR RAHMAN[1], SUBRATA K. SARKER[2], SAJAL K. DAS[1], MD. RABIUL ISLAM[3], (Senior Member, IEEE), ABBAS Z. KOUZANI[4], AND M. A. PARVEZ MAHMUD[4]

[1]Department of Mechatronics Engineering, Rajshahi University of Engineering & Technology, Rajshahi 6204, Bangladesh
[2]Department of Electrical and Electronic Engineering, Varendra University, Rajshahi 6204, Bangladesh
[3]Faculty of Engineering and Information Sciences, University of Wollongong, Wollongong, NSW 2522, Australia
[4]School of Engineering, Deakin University, Geelong, VIC 3216, Australia

Corresponding author: Mizanur Rahman (mizan138027@gmail.com)

ABSTRACT This paper presents the design of an extended parameterisations of H_∞ controller for off grid operation of a microgrid. The microgrid consists of distributed generation units, filters and local loads. The filters are used to achieve accurate sinusoidal output voltage. However, loads which are connected to the microgrid are parametrically uncertain. Hence, it undergoes with unknown loads uncertainties. These unknown loads may create unknown loads harmonics, non-linearities which may reduce the voltage and current profile of the microgrid. As a result, the sudden rise and fall of voltage current profile damages the domestic and commercial loads. The proposed controller provides robust stability against various unknown loads and uncertainties. The design of the controller is presented using linear matrix inequality approach and satisfies the Lyapunov stability criterion. Moreover, it provides lower closed-loop H_∞ norm and has better tracking accuracy than other. For justification, several load conditions have been tested in MATLAB/SimPowerSystem Toolbox to ensure the robust stability of the proposed controller. All the results presented in the paper indicate high performance of the controller.

INDEX TERMS Microgrid, voltage control, LMI, H_∞ controller.

I. INTRODUCTION

The use of continuous power, without depending on the fuels, gasses and oils, leads people to renewable and distributed generation (DG) technology. As the insufficiency and increasing cost of fossil fuel, researchers are more and more interested on DG units [1]. Microgrid (MG) is defined as generation of electricity by the facilities that are smaller than central generating plants and allows interconnection nearly at any point in the power system [2], [3]. The distributed power systems are structured by input power sources with different configurations. Such DG units are wind turbines, combined heat and power (CHP), photovoltaic systems, and hydroelectric systems. These DG units are connected to the MG via a voltage source inverter (VSI). To improve the performance at lower switching frequencies, an output filter is connected in series with the inverters [4]. Consequently, power obtaining through these DGs is difficult to predict which do not coincide with the power demand. For this problem, energy storage systems are required to supply continuous power to the local load.

MGs are integration of various power systems [5] and are considered as local grid and consist of generators, loads and energy storage elements. An illustration of a MG is shown in Fig. 1. The operation of MG follows grid connected technique and stand-alone method [6]. In grid connected technique, distributed energy sources (DERs) help the utility grid on the contrary rest is connected to the MG at the point of common connection (PCC) [7]. In stand-alone technique, the MG is disconnected from main grid and can be supplied uninterruptible power to the load [8]. The disconnection is occurred because of large disturbances such as: fault, poor power quality, and voltage deterioration.

In the configuration of grid mode, frequency and voltage of the system are being determined by transmission grid and MG can deliver power to the main grid or it can take power from

The associate editor coordinating the review of this manuscript and approving it for publication was Siqi Bu.

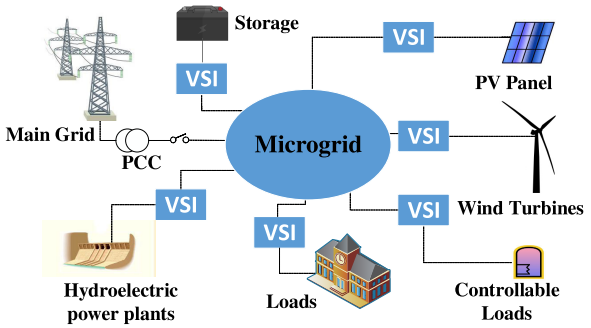

FIGURE 1. An illustration of a microgrid system.

main grid [9]. MG can reduce the feeder losses, increases the energy efficiency, facilitates the uses of renewable energy, reliability and support local voltage. Islanded MG can be used in remote places in case of the absence of main grid or for the complexity of extracting power from main grid [10].

Control strategies of the voltage and frequency depend on the balance of the active and reactive power. New ideas are created for the coordinated operation of the distributed energy resources with the MG concept. According to the Consortium for Electric Reliability Technology Solutions (CERTS), heat and power both are provided by MG [6], [11]–[13].

A common phenomenon known as low frequency inter-area power oscillations is raised between the interconnection of rotating generators or between weak or heavy load AC inertias. This phenomenon is caused by line fault, switching of lines or sudden change of generator output. The typical range of this oscillating frequencies lies in $< 2Hz$, and creates self-control power transmission capability. This power oscillation damping increases power transmission capability and hence, the power oscillation damping is important.

A. LITERATURE REVIEW

Though a DG unit can not generate exactly $50Hz$ or $60Hz$ voltage, it is connected to the main grid with a VSI [14]. So the control of VSI is very important. To obtain the satisfactory performance for the control of MG voltage, a number of controllers have been used [12], [13], [17]. The voltage of the plant can be controlled by applying linear quadratic regulator (LQR) [15]. It is used to obtain better voltage regulation and simultaneous load sharing. The performance of a LQR controller depends on plant transfer function. For a fixed transfer function, the performance of the controller is very high. However, a number of disturbances such as nonlinear load, unknown load, and harmonic load can change the plant dynamics. Proportional integral derivative (PID) controller is mostly used in industry applications [15]. The advantages of this controller are simplicity to design, high bandwidth, and almost zero error voltage tracking performance [16]. Moreover, this controller can ensure fast response time, and negligible overshoot. Besides, it is applicable for linear time-invariant single-input, and single-output system.

Hysteresis controller is used for current regulation of MG. It is a current control method which is used to control the VSI. As a current controller, the grid current follows a reference current [18]. The advantages of this controller are simplicity, robustness and good transient response [19]. But the switching frequency with respect to the load parameters is the main drawback of the controller [20].

For a high dynamic and first transient response, a deadbeat controller (DBC) can be used widely in different applications [21], [22]. It provides a control scheme to maintain the current in a nominal range. The DBCs are feedback controller and the gain of the controller is based on the plant system order. It provides zero steady-state error, minimum rise and settling time with less then 2% overshoot, and high control output. The controller is suitable where the plant parameters are fixed and can provide desired performance using a fixed model of filter.

A droop control method has been proposed to stabilize the grid voltage and frequency [15]. The design of the controller is derived from a simple proportional controller. The controller gain selection depends on power balancing criteria. It enables the use of more inverters in interconnected mode. Moreover, active and reactive power balance in power system can be achieved from this control technique [23]–[26]. For power sharing, a static droop compensator is already used in literature [23], [24]. It controls the active and reactive power on the basis of frequency and voltage droop control methods respectively.

Predictive controller is designed for controlling the converters with disturbances and periodic reference signal [27], [28]. This controller can predict and minimize the periodic error at the beginning of each sample. At all frequencies, it provides zero steady state error. In most applications, a predictive controller can ensure robust tracking performance. However, this controller requires a mathematical approach and sensitive to parameter change.

Improvement of voltage oscillation, compensation for unwanted harmonics, tracking of command voltages and quality control of power profile of MG particularly for islanded mode operation using modern control techniques have been the area of continuous research which can be seen in the references [32]–[34] and so forth. The work presented in [35], [36] and the works presented in the paper are completely different in the spectrum of control designs. The aim of the design of the controller is different in the context of the paper presented in [35], [36]. The design of the controller presented in [35] is carried out to track the command voltages only of single phase islanded MG whereas the controller presented in [36] is designed to reduce the unwanted voltage oscillation and harmonics for both single and three phase MG by damping the resonant modes of the system. However the design of the controller presented in the current work is done to compensate for the voltage oscillation, unwanted harmonics and follow the command voltages simultaneously for both single and three phase operation of islanded MG. The modeling of the test system remains same to justify the

unique performance of the controller designed in the current work.

B. CONTRIBUTION AND PAPER ORGANIZATION

In a power system, it is desired to have a low order controller to reduce the complexity of the power system implementation. It is also important to maintain closed-loop stability against a number of uncertainties. Due to the uncertainties of a MG system such as parameter and load variation, the regulation of a three phase voltage/current is more challenging than controlling of a single phase MG. Moreover, in a three phase MG, the deviation of voltage/current in one phase affects the other phases.

In this paper, we present the design of an H_∞ controller for voltage, current and power stabilization of the islanded MG. An LMI based framework that shows robustness in a greater spectrum as compared to the conventional H_∞ design presented in [29]–[31] has been developed to function the controller. The novelty and contribution of the current work in terms of the control perspective is the design of control framework. The designed framework has been devised by taking into account to direct multiple control variables e.g., voltage, current and power simultaneously. This is important because design of a controller to manipulate single control variable may have undesirable consequences on other control variables of the plant and doing so does not certify the robustness of the overall closed-loop system.

In terms of power point of view, since the controller is designed to supervise multiple variables concurrently, it ensures quality profile of voltages, currents and power all together using single a controller instead of designing several controllers which sequentially reduces the complexity of the overall system in addition.

The remainder of this paper is organised as follows: Section II represents the modeling of the MG. The control framework is described in Section III. Section IV provides a performance evaluation, while Section V concludes the paper.

II. MODELING OF THE ISLANDED MICROGRID

A. MICROGRID CONFIGURATION

Fig. 2(a) shows a single phase energy source MG configuration for analysing and evaluating the performance of the MG system. It has DC voltage source V_{dc}, LC filter, voltage source inverter (VSI) and line and load impedance. The VSIs are used in between grid network and DC voltage source to transfer power from DC side to AC side. In steady state condition, the average AC power P_{ac} is equal to DC power P_{dc}. IGBTs are used to comprise the VSI and the switching action of each IGBT is defined by $V_{sw} = \delta V_{dc}$, where δ is the duty ratio with $\delta \in [-1,\ 1]$. However, as power solid state devices have little switching ripple, LC filters are used to attenuate this ripple.

The three phase MG also has similar components excepts transformers which is shown in Fig. 2(b). The power transformers are used to transmit power from Distributed generation station to medium-voltage line in order to reduce the line losses and transmission cost. As loads parameters are uncertain, they create fluctuations and high frequency harmonics. The shunt capacitor C_{st} is used to attenuate this high frequency harmonic impact. Moreover, a crystal oscillator (i.e. internal oscillator) is used for the purpose of controlling the MG frequency in an open-loop control manner with $w_o = 2\pi \times f,\ f = 60\ Hz$.

B. VOLTAGE CONTROL

The block diagram for the voltage control of a MG system is shown in Fig. 2. The desired grid voltage v_g for each VSI is tracked by the voltage control loop. The switching frequency of VSI depends on a duty ratio δ which is very important to achieve accurate voltage tracking performance. This duty ratio is determined by the controller with $\delta \in [-1, 1]$ using pulse width modulation (PWM) principle. In a voltage control loop, the grid voltage is provided by the VSI which is compared with the desired reference MG voltage. Moreover, for voltage tracking performance, the control loop requires a high bandwidth.

C. MODELING OF SINGLE PHASE MICROGRID

For the modeling of single phase MG, the inductor current i_L in the L-C filter (Fig. 2(a)) is divided into filter capacitor current i_c and grid current i_g. The controller design is based on-

$$L_t \frac{di_L(t)}{dt} = v_{sw} - v_g(t) \tag{1}$$

The switching voltage v_{sw} over a pulse width modulation is written as

$$v_{sw} = \tau v_{dc} \tag{2}$$

For grid voltage v_g

$$C_{st} \frac{dv_g}{dt} = i_c \tag{3}$$

From (1) and (3), the derived state-space model of the single phase MG is as follows

$$\frac{dx}{dt} = Ax + Bu + dw \tag{4}$$

$$y = Cx + Du \tag{5}$$

where, x, u, and w are the state vector, input vector, and exogenous input vector of the MG, respectfully. Also, the disturbances d next to the state vector and input vector are considered. The disturbances, due to unknown configuration of MG, are associated with the grid current. The state vector, input vector and exogenous input vector of the MG are as follows

$$x = \begin{bmatrix} i_L \\ v_g \end{bmatrix};\quad u = \begin{bmatrix} v_{sw} \end{bmatrix};\ d = \begin{bmatrix} i_g \end{bmatrix}$$

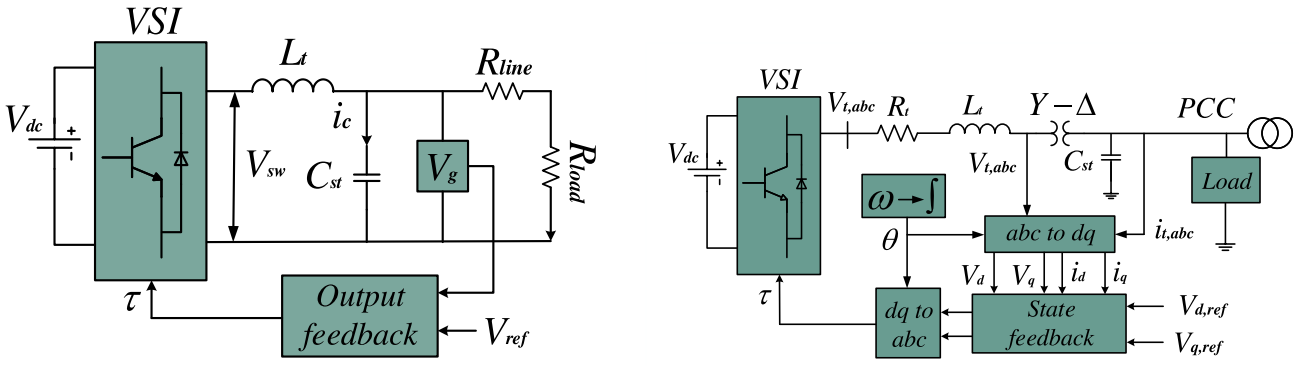

FIGURE 2. Closed-loop voltage/current control strategy of (a) single phase single energy source microgrid system, (b) three phase single energy source microgrid.

And the state space of the system is as follows

$$\frac{d}{dt}\begin{bmatrix} i_L \\ v_g \end{bmatrix} = \begin{bmatrix} 0 & -\frac{1}{L_t} \\ \frac{1}{C_{st}} & 0 \end{bmatrix}\begin{bmatrix} i_L \\ v_g \end{bmatrix} + \begin{bmatrix} \frac{1}{L_t} \\ 0 \end{bmatrix}\begin{bmatrix} v_{sw} \end{bmatrix} + \begin{bmatrix} 0 \\ -\frac{1}{C_{st}} \end{bmatrix}\begin{bmatrix} i_g \end{bmatrix} \quad (6)$$

The output of the system is defined as

$$\begin{bmatrix} y \end{bmatrix} = \begin{bmatrix} v_g \end{bmatrix} = \begin{bmatrix} 0 & 1 \end{bmatrix}\begin{bmatrix} i_L \\ v_g \end{bmatrix} \quad (7)$$

D. MODELING OF THREE PHASE MICROGRID

The modeling of three phase MG is illustrated in Fig. 2(b). The governing equation of the open-loop system can be defined in abc-frame as follows

$$v_{t,abc} = L_t \frac{di_{t,abc}}{dt} + R_t i_{t,abc} + v_{abc} \quad (8)$$

$$i_{t,abc} = C_{st} \frac{dv_{abc}}{dt} \quad (9)$$

The transformation of the dynamic system in (8)-(9) from abc-frame to $\alpha\beta$-reference frame is derived as

$$di_{t,\alpha\beta} = -\frac{R_t}{L_t} i_{t,\alpha\beta} - \frac{v_{\alpha\beta}}{L_t} + \frac{v_{t,\alpha\beta}}{L_t} \quad (10)$$

$$dv_{\alpha\beta} = \frac{i_{t,\alpha\beta}}{C_{st}} \quad (11)$$

Finally, the above equations in (10)-(11) are transformed to dq-rotating frame and the resultant equations are presented as

$$\frac{dI_{t,dq}}{dt} + sI_{t,dq} = -\frac{R_t}{L_t} I_{t,dq} + \frac{1}{L_t} V_{t,dq} - \frac{1}{L_t} V_{dq} \quad (12)$$

$$\frac{dV_{dq}}{dt} + sV_{dq} = \frac{1}{C_{st}} I_{t,dq} \quad (13)$$

where, $s = jw_o$. The state-space representation of the open-loop three phase MG in (12)-(13) is written as $G_P(s) = C_P(sI - A_P)^{-1}B_P + B_w + D_P$, and the state matrices are defined as

$$A_P = \begin{bmatrix} 0 & \omega_o & \frac{1}{C_{st}} & 0 \\ -\omega_o & 0 & 0 & \frac{1}{C_{st}} \\ -\frac{1}{L_t} & 0 & -\frac{R_t}{L_t} & \omega_o \\ 0 & -\frac{1}{L_t} & \omega_o & -\frac{R_t}{L_t} \end{bmatrix},$$

$$B_P = \begin{bmatrix} 0 & 0 \\ 0 & 0 \\ \frac{1}{L_t} & 0 \\ 0 & \frac{1}{L_t} \end{bmatrix}$$

$$B_w = \begin{bmatrix} -\frac{1}{C_{st}} & 0 \\ 0 & -\frac{1}{C_{st}} \\ 0 & 0 \\ 0 & 0 \end{bmatrix}, \quad C_p = \begin{bmatrix} 1 & 0 & 0 & 0 \\ 0 & 1 & 0 & 0 \end{bmatrix}$$

and $D_p = 0$

Here $x = \begin{bmatrix} V_d & V_q & I_{td} & I_{tq} \end{bmatrix}^T$ is the state vector; $u = \begin{bmatrix} V_{td} & V_{tq} \end{bmatrix}^T$ is input vector, $w = \begin{bmatrix} i_{Ld} & i_{Lq} \end{bmatrix}^T$ is the exogenous input vector and the output vector is defined as $y = \begin{bmatrix} V_d & V_q \end{bmatrix}$.

The system parameter values for the three phase MG system are given in Table 1.

III. DESIGN OF THE CONTROLLER

A. PRELIMINARY DEFINITIONS

Prior to the design of the proposed controller for the MG, this section represents some preliminaries of extended parameterisations of H_∞ norms which are more detailed in [38]. Now, consider the LTI discrete system with a state-space representation as

$$x(m+1) = Ax(m) + Bw(m) \quad (14)$$

TABLE 1. Parameters of microgrid system.

Parameters	Single phase MG	Three phase MG
DC bus voltage v_{dc}	$300V$	$2000V$
Shunt capacitance (C_st)	$15\mu F$	$100\mu F$
Inductor filter	$2mH$	2.53
Line resistance (R_{line})	0.45 Ω	
Consumer load (R)	40 Ω	
Frequency (f)	60Hz	60Hz
VSC terminal voltage (line-line) (V_{base})		$600V$ (1 pu)
Transformer voltage ratio (Y/Δ)		0.6/13.8
PWM carrier frequency (f_{sw})		1980 Hz
VSC filter resistance (R_t)		$1.5m\Omega$
DG rated power (S_{base})		$3MVA$(1 pu)

$$q(m) = Cx(m) + Dw(m) \tag{15}$$

where x, w, and q are defined as a state vector, the exogenous input, and the controlled output respectively. The other vectors and matrices are in proper dimensions. The system in (14)-(15) is asymptotically stable if it satisfies the following LMI

$$A^T\mathcal{L} + \mathcal{L}A < 0 \tag{16}$$

such that $\mathcal{L} > 0$

where $\mathcal{L}$ is a real positive definite matrix. If $\mathcal{L}$ is the positive definite then the system $x = Ax(m)$ is asymptotically stable, that is all the eigenvalues of A satisfy $\mathbb{R}\lambda_i < 0$.

However, the LMI in (16) has been modified by including another matrix $\mathcal{M} \in \mathbb{R}^{n\times n}$ such that the following inequality

$$\begin{bmatrix} \mathcal{L} & A\mathcal{M} \\ \mathcal{M}^T A & \mathcal{M} + \mathcal{M}^T - \mathcal{L} \end{bmatrix} > 0 \tag{17}$$

is feasible.

The extended stability criterion in (17) is generalised to calculate the H_∞ norm for the development of state-feedback and output-feedback controller [39].

Lemma (H_∞ Norm) [38]: There exists a real positive semi-definite matrix $\mathcal{L}$ such that $||H_{wq}(s)||_\infty^2 < \eta$ holds if, and only if, the following LMI

$$\begin{bmatrix} \mathcal{L} & A\mathcal{L} & B & 0 \\ \mathcal{L}A^T & \mathcal{L} & 0 & \mathcal{L}C^T \\ B^T & 0 & I & D^T \\ 0 & C\mathcal{L} & D & \eta I \end{bmatrix} > 0 \tag{18}$$

is feasible.

Theorem 1: There exists a real positive semi-definite matrix $\mathcal{L}$ and a matrix $\mathcal{M}$ such that $||H_{wq}(s)||_\infty^2 < \eta$ holds

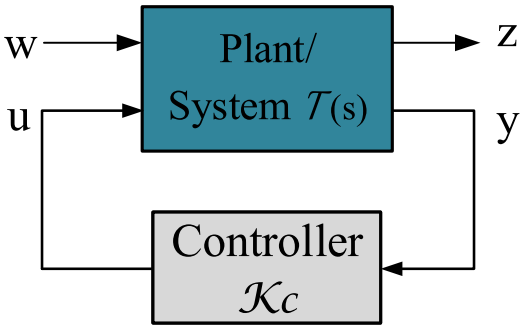

FIGURE 3. Block diagram of the closed-loop system.

if, and only if, the following LMI

$$\begin{bmatrix} \mathcal{L} & A\mathcal{M} & B & 0 \\ \mathcal{M}A^T & \mathcal{M} + \mathcal{M}^T - \mathcal{L} & 0 & \mathcal{M}^T C^T \\ B^T & 0 & I & D^T \\ 0 & C\mathcal{M} & D & \eta I \end{bmatrix} > 0 \tag{19}$$

is feasible.

Theorem 2: If the system matrix Ψ_i belong to a polytropic set φ, where

$$\Psi_i = \begin{bmatrix} A_i & B_i \\ C_i & D_i \end{bmatrix}, \quad i = 1, 2, \ldots, N \tag{20}$$

Then there exists a matrix $\mathcal{M}$ and a real positive semi-definite matrix $\mathcal{L}$ such that $||H_{wq}(s)||_\infty^2 < \eta$ holds if, and only if, the following LMI

$$\begin{bmatrix} \mathcal{L}_i & A_i\mathcal{M} & B_i & 0 \\ \mathcal{M}A_i^T & \mathcal{M} + \mathcal{M}^T - \mathcal{L}_i & 0 & \mathcal{M}^T C_i^T \\ B_i^T & 0 & I & D_i^T \\ 0 & C_i\mathcal{M} & D_i & \eta I \end{bmatrix} > 0 \tag{21}$$

is feasible.

B. LMI SYNTHESIS FOR STATE-FEEDBACK CONTROLLER

Consider a LTI system $\mathcal{T}(s)$ in Fig. 3 which can be represented as

$$x_{op}(m) = A_{op}x_{op} + B_1 w + B_2 u \tag{22}$$
$$q(m) = C_1 x_{op} + D_{11} w + D_{12} u \tag{23}$$
$$y(m) = C_2 x_{op} + D_{21} w + D_{22} u \tag{24}$$

where, $x_{op} \in \mathbb{R}^n$ is the state vector, $A_{op} \in \mathbb{R}^{n\times n}$ is the system matrix and y is the measured output. The control input, and controlled output are defined as u and q, respectively and all other matrices and vectors are in proper dimension.

The above system maps the inputs $\begin{pmatrix} w \\ u \end{pmatrix}$ to control the outputs $\begin{pmatrix} q \\ y \end{pmatrix}$ i.e.

$$\begin{pmatrix} q \\ y \end{pmatrix} = \mathcal{T}(s) \begin{pmatrix} w \\ u \end{pmatrix} \tag{25}$$

The interconnection of the system with the controller $\mathcal{K}_c$ will produce a linear closed-loop system which has a state-space representation as follows

$$x_{cl}(m) = A_{cl}x_{cl} + B_{cl}w \tag{26}$$
$$q(m) = C_{cl}x_{cl} + D_{cl}w \tag{27}$$

The control problem is to find the full state-feedback and output-feedback controller $\mathcal{K}_c$ with which the system in (22)-(24) generates a LTI system like in (26) and (27) to map the exogenous input w to control output q such that the system in (22) is internally stable. The maximum gain from w to q is less than H_∞ norm parameter ϑ. Moreover, it reduces the high frequency noises and disturbances of the voltage source converter and tracks the reference signal.

1) FULL STATE-FEEDBACK CONTROLLER

For the development of extended parameterizations of the H_∞ full state-feedback controller, the states of the system must be available to feed the controller. In addition to consider the information of the states are not corrupted by the exogenous input w. As a result, there will be a control law in the form of

$$u = Kx \tag{28}$$

where the closed-loop system matrices are defined as follows

$$A_{cl} = A_{op} + B_2\mathcal{K}_c, \quad B_{cl} = B_1 \tag{29}$$
$$C_{cl} = C_1 + D_{12}, \quad D_{cl} = D_{11} \tag{30}$$

Moreover, practical systems in (22)-(24) are uncertain. For the development of the robust stable controller assume that the system matrix Ψ belongs to a convex bounded polyhedron set φ such that

$$\varphi := \Psi(\delta) : \Psi(\delta) = \sum_{i=1}^{N} \delta_i \Psi_i, \quad \delta_i = 1, \sum_{i=1}^{N} \delta_i = 1 \tag{31}$$

where, $\Psi_i = \begin{bmatrix} A_{op} & B_1 & B_2 \\ C_1 & D_{11} & D_{12} \end{bmatrix}$
with, $\Psi_i = \{\Psi_1, \ldots\ldots, \Psi_N\}$

Now, using the change of variable in theorem (19)-(20) as

$$\mathcal{L} = L, \quad \mathcal{M} = Y, \text{ and } P = \mathcal{K}_c Y$$

the proposed state-feedback controller is constructed. To design the controller in the form of (28), there exist symmetric matrices Y, P and L_i such that the H_∞ norm $||H_{wz}(s)||_\infty^2 < \eta$ satisfies the following LMI

$$\begin{bmatrix} L_i & A_{op,i}Y + (B_{12})_i P & (B_{11})_i & 0 \\ * & Y + Y^T - L_i & 0 & Y^T(C_1)_i^T + P^T D_{12}^T \\ * & * & I & D_{11}^T \\ * & * & * & \eta I \end{bmatrix} > 0 \tag{32}$$

And the state-feedback gain can be calculated as

$$\mathcal{K}_c = PY^{-1} \tag{33}$$

2) FULL OUTPUT-FEEDBACK CONTROLLER

Consider a linear output-feedback controller $\mathcal{K}_c$ which has a state-space representation as follows

$$x_c(m) = \mathcal{A}_c x_c + \mathcal{B}_c y_c \tag{34}$$
$$u(n) = \mathcal{C}_c x_c + \mathcal{D}_c y_c \tag{35}$$

where, the controller state vector is defined as $x_c \in \mathbb{R}^n$. While connecting this controller with the system in (22)-(24) produces a linear system in the form of (26)-(27), where the closed-loop state vector and matrices are defined respectively as follows

$$\bar{x}(n) = \begin{bmatrix} x(m) \\ x_c(m) \end{bmatrix} \tag{36}$$
$$A_{cl} = \begin{bmatrix} A_{op} + B_{12}\mathcal{D}_c C_2 & B_{12}\mathcal{C}_c \\ \mathcal{B}_c C_2 & \mathcal{A}_c \end{bmatrix},$$
$$B_{cl} = \begin{bmatrix} B_2 + B_1\mathcal{D}_c D_{21} \\ \mathcal{B}_c D_{21} \end{bmatrix} \tag{37}$$
$$C_{cl} = \begin{bmatrix} C_1 + D_{12}\mathcal{D}_c C_2 & D_{12}\mathcal{C}_c \end{bmatrix},$$
$$D_{cl} = \begin{bmatrix} D_{11} + D_{12}\mathcal{D}_c D_{21} \end{bmatrix} \tag{38}$$

For the development of output-feedback controller in the form of (34)-(35), there exist the matrices Y, P, $\mathcal{Y}$, F, Q, R, S, J and the symmetric variable matrices P and H such that the H_∞ norm of the closed-loop system $||H_{wz}(s)||_\infty^2 < \eta$ holds, if and only if the inequality in (39), as shown at the bottom of the next page is satisfied and the robust output-feedback controller can be obtained as

$$\begin{bmatrix} A_c & B_c \\ C_c & D_c \end{bmatrix} = \begin{bmatrix} V^{-1} & V^{-1}\mathcal{Y}B_2 \\ 0 & I \end{bmatrix} \begin{bmatrix} Q - \mathcal{Y}AY & F \\ L & R \end{bmatrix} \times \begin{bmatrix} U^{-1} & 0 \\ -C_2 Y U^{-1} & I \end{bmatrix} \tag{40}$$

where $UV + \mathcal{Y}Y = S$.

C. PARAMETER ESTIMATION OF THE CONTROLLER

This section shows the controller parameters of the state feedback and output feedback controller. Using the parameters of the single and three phase MG in Table 1 and LMI's in (32), (33), (39), (40), the controllers are constructed which are used to regulate voltage and current profile of the MG systems. Moreover, H_∞ norms show how far the estimated voltage and current from the desired values.

Both the aforemention control approaches, output-feedback and state-feedback, can be used to control the MG operations. However, in a single-phase MG, the MG operation is concluded with voltage control (Fig. 2(a)). But the states i.e. voltage and current, have impact on three-phase MG (Fig. 2(b)). The control parameters are given as follows

1) PARAMETERS FOR SINGLE-PHASE MICROGRID

Now, using the LMI Control Toolbox in MATLAB, the output-feedback controller in (40) is constructed by

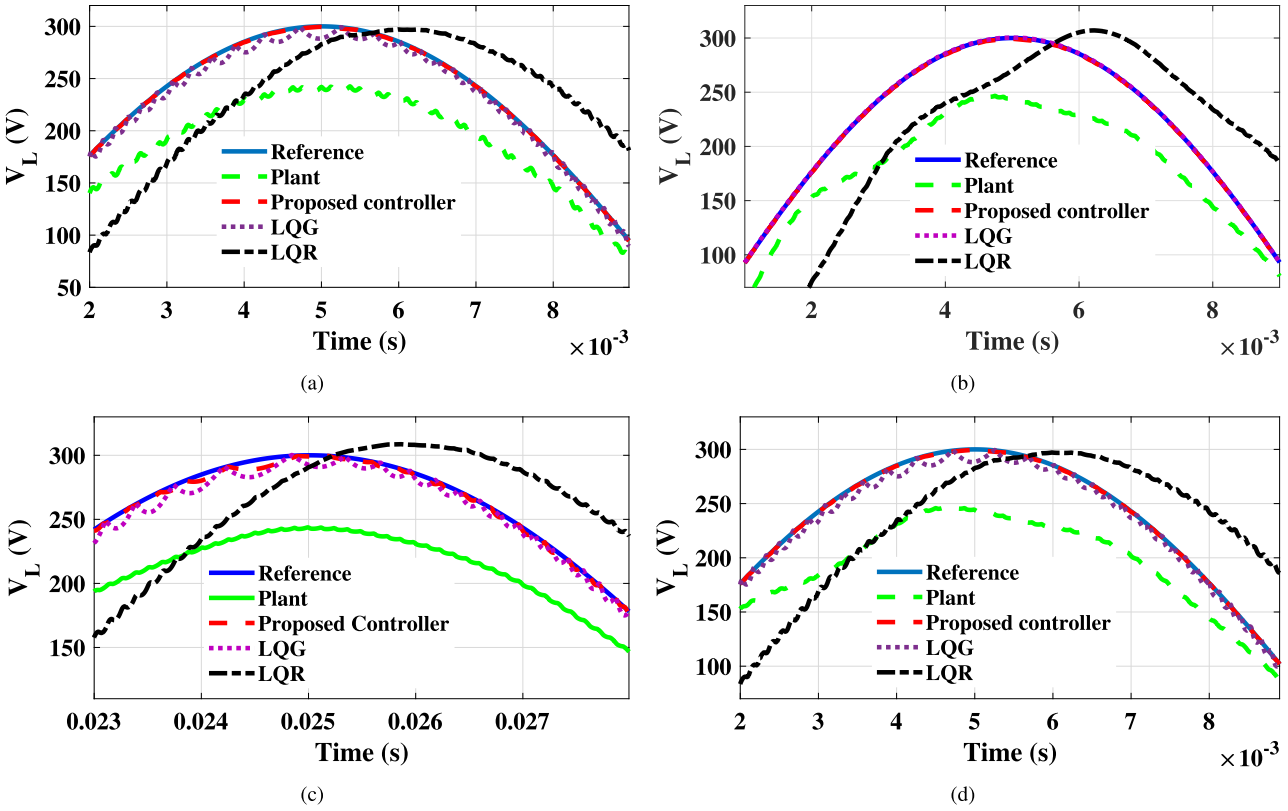

FIGURE 4. Voltage tracking performance of microgrid under (a) Consumer load, (b) Unknown load, (c) Harmonic load, (d) Non-linear load (The green dashed (−−), blue solid (–), red dashed (−−), purple doted (..), and black curved line represent the open-loop, reference signal, proposed controller, linear quadratic gaussian (LQG) controller, and LQR controller respectively).

solving the LMI in (39)

$$A_c = 1 \times 10^4 \begin{bmatrix} 0.0 & -4.1036 \\ 0.0 & 0.0009 \end{bmatrix},$$
$$B_c = 1 \times 10^{-3} \begin{bmatrix} -0.4320 \\ -0.0001 \end{bmatrix} \quad (41)$$
$$C_c = \begin{bmatrix} 0.0 & 0.0350 \end{bmatrix} \quad D_c = 1 \quad (42)$$

where $\eta = 1.5$ and

$$||H_{wz}(s)||_\infty^2 < \eta = 1.1$$

The controller is designed to deal with the real scenarios of the islanded MG and practical implementation of the controller is not the scope of the current work.

2) PARAMETERS FOR THREE-PHASE MICROGRID

For the three phase MG system, the matrices P and Y are constructed from the LMI in (32) as

$$P = 1 \times 10^8 \begin{bmatrix} 3.6224 & 0.0 & -0.0 & 0.1138 \\ 0.0 & 3.6202 & -0.1137 & 0.0 \\ -0.0 & -0.1137 & 0.0036 & -0.0 \\ 0.1138 & 0 & -0.0 & 0.0036 \end{bmatrix} \quad (43)$$
$$Y = 1 \times 10^8 \begin{bmatrix} 3.6188 & -0.0002 & 0.0 & 0.1137 \\ 0.0002 & 3.6237 & -0.1138 & 0.0 \end{bmatrix} \quad (44)$$

where $\eta = 1.5$

Then, the state-feedback gain from (33) is calculated as

$$F = \begin{bmatrix} 1.0010 & 0.0 & 0.0005 & -0.0628 \\ 0.0 & 1.0010 & 0.0 & 0.0015 \end{bmatrix}$$
$$||H_{wz}(s)||_\infty^2 < \eta = 1.2345 \quad (45)$$

$$\begin{bmatrix} L & J & A_{op}Y + B_2P & A_{op} + B_2RC_2 & B_1 + B_2RD_{21} & 0 \\ * & H & Q & \mathcal{Y}A_{op} + FC_2 & \mathcal{Y}B_2 + FD_{21} & 0 \\ * & * & Y + Y^T - L & I + S^T - J & 0 & Y^TC_1^T + \mathcal{L}^TD_{12}^T \\ * & * & * & \mathcal{Y} + \mathcal{Y}^T - H & 0 & C_1^T + C_2^TR^TD_{12}^T \\ * & * & * & * & I & D_{11}^T + D_{21}^TR^TD_{12}^T \\ * & * & * & * & * & \eta I \end{bmatrix} \geq 0, \quad (39)$$

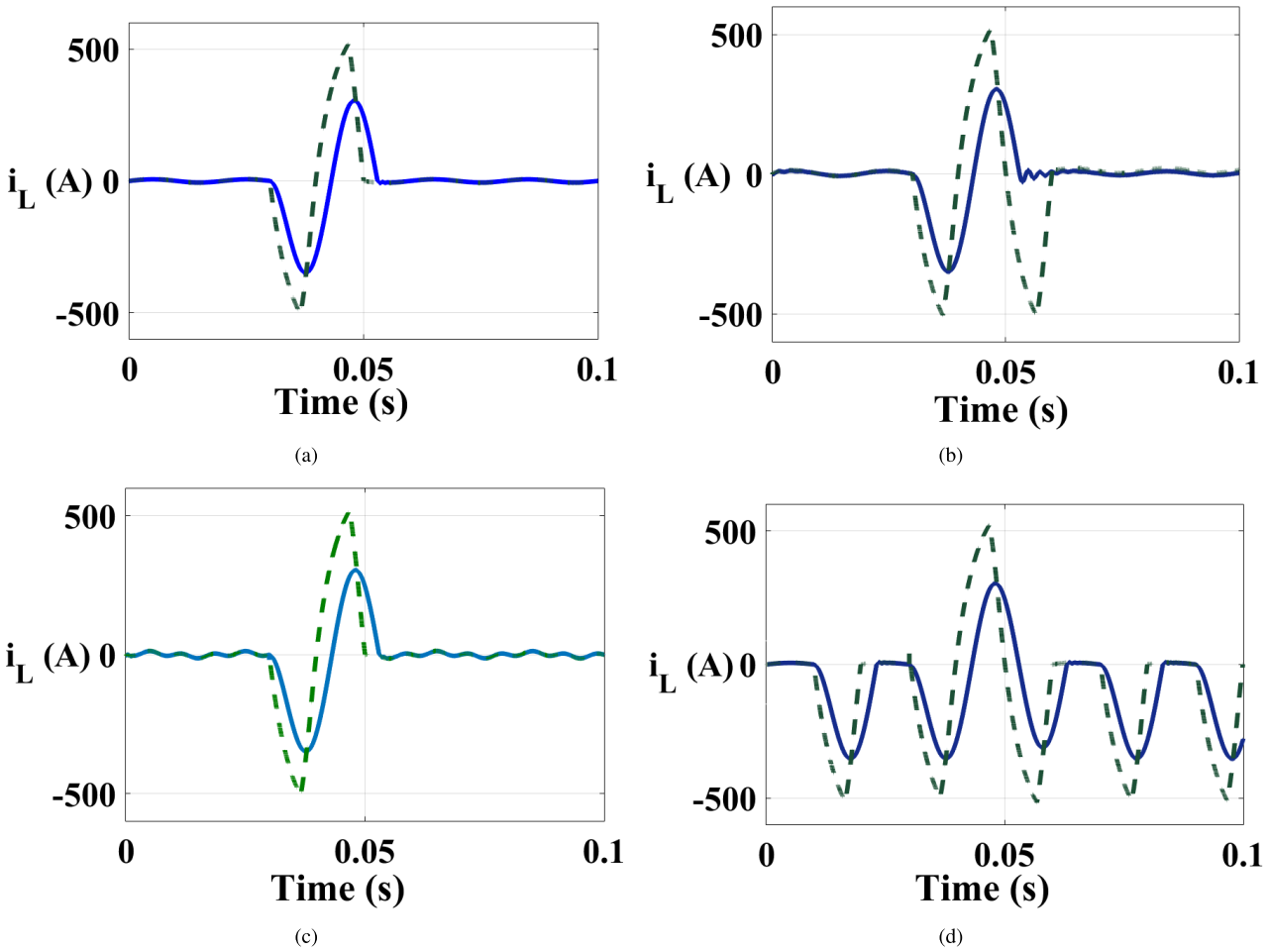

FIGURE 5. Fault current tracking performance of microgrid under (a) Consumer load, (b) Unknown load, (c) Harmonic load, (d) Non-linear load (The green dashed (−−), blue solid (−) line represent the open-loop and closed-loop response respectively).

IV. PERFORMANCE EVALUATION

The performance of the introduced controller for both single and three phase MG system is represented in this section. The effectiveness of the controller may deviate due to increasing number of subsystem in the MG. Each of the subsystems consists of a energy source that will increase the number of control variable for the MG. As a result, the control of a three phase MG system is more challenging than single phase system. The proposed H_∞ controller is successful to regulate the voltage and current of MG. The results of this section are obtained using MATLAB/SimPowerSystem Toolbox which indicate the robust stability and performance of the controller.

A. PERFORMANCE EVALUATION FOR SINGLE PHASE MICROGRID

For the performance evaluation of the single phase MG, the DC bus voltage, line and load resistance are considered as 300 V, $R_{line} = 3\Omega$ and $R_{load} = 40\Omega$, respectively. For the LC filter, the parameters are: $C = 15\mu F$ and $L = 2mH$. The performances against consumer load are shown in Fig. 4, and 5 which indicate high performance of the controller. The robustness of the proposed controller under different load conditions are given below:

1) PERFORMANCE AGAINST UNKNOWN LOAD

The performance of single phase MG is affected by unknown loads. Fig. 6(a) shows an unknown load circuit that is connected in parallel with the MG. When the switch of the circuit is closed then the steady state, capacitance, inductance and resistance value of the circuit will also change. Initially, the switch in Fig. 6(a) is opened but at $t = 0.36$ sec the unknown load is connected to the grid and the performance is evaluated. The performance of the controller against the unknown load is shown in Fig. 4(b), and 5(b). The results show that the proposed controller ensure the highest tracking performance against unknown load.

2) PERFORMANCE AGAINST HARMONIC LOAD

The non-linear loads are responsible to produce harmonics which cause distortion in voltage and current. Fig. 6(b) shows a harmonic load circuit. The harmonic voltage and current generate an increased amount of heat in loads and conductors. This phenomenon may damage the performance and

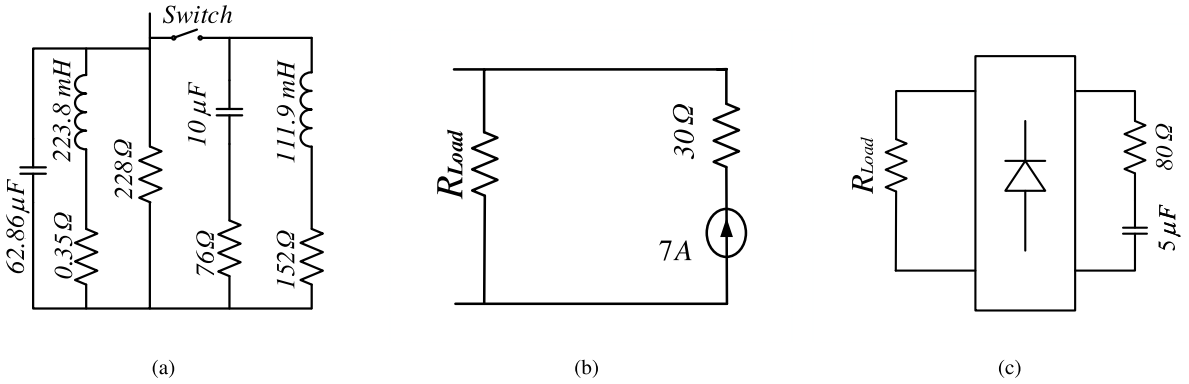

FIGURE 6. Simulation circuit diagram of (a) Unknown load, (b) Harmonic load, (c) Non-linear load (for a single phase).

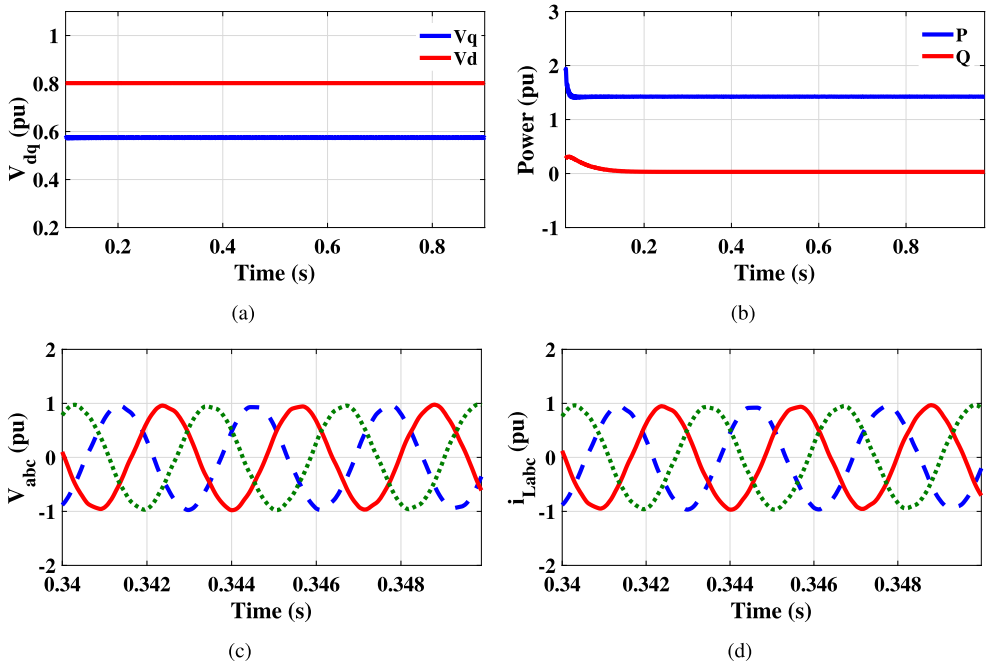

FIGURE 7. Simulation results of the proposed controller: (a) d and q components of the load voltage, (b) power components, (c) instantaneous load voltages and their magnitude (solid red (–) line phase a, dashed blue (––) line phase b, and doted green (..) line phase c), (d) instantaneous load currents and their magnitude (solid red (–) line phase a, dashed blue (––) line phase b, and doted green (..) line phase c).

durability of the loads. The waveform of the current depends on the loads. Due to the source impedance and non-linear loads, the source voltage will be affected. Hence, the quality of the voltage will be deteriorated. The main problem caused by the harmonic loads is the increased system's current which is an order of $3rd$ harmonics. To produce a current waveform of $3rd$ order harmonics of amplitude $7A$ and frequency $150Hz$, a 30Ω resistor is connected in series to the current source. The voltage tracking performance of the controllers under harmonic loads is presented in Fig. 4(c), and 5(c). The results show that the proposed H_∞ controller shows robust performance against the harmonic load.

3) PERFORMANCE AGAINST NON-LINEAR LOAD

This test is to verify the stability and robustness of the proposed controller. A non-linear load circuit is shown in Fig. 6(c) and the dynamic performance of the controller against non-linear load is shown in Fig. 4(d), and 5(d). A two phase four pulse diode bridge rectifier with RC load is considered as a non-linear load for this simulation. The load is connected in parallel with the grid load (R_{load}). From the simulation results, it has been seen that the proposed controller provides a negligible voltage tracking performance error with an acceptable total harmonic distortion.

B. PERFORMANCE EVALUATION FOR THREE PHASE MICROGRID

The effectiveness of the controller against consumer load is determined by considering reference voltages $V_d = 0.8\ pu$ and $V_q = 0.6pu$. The dynamic performance against the consumer loads is presented in Fig. 7. The results show that

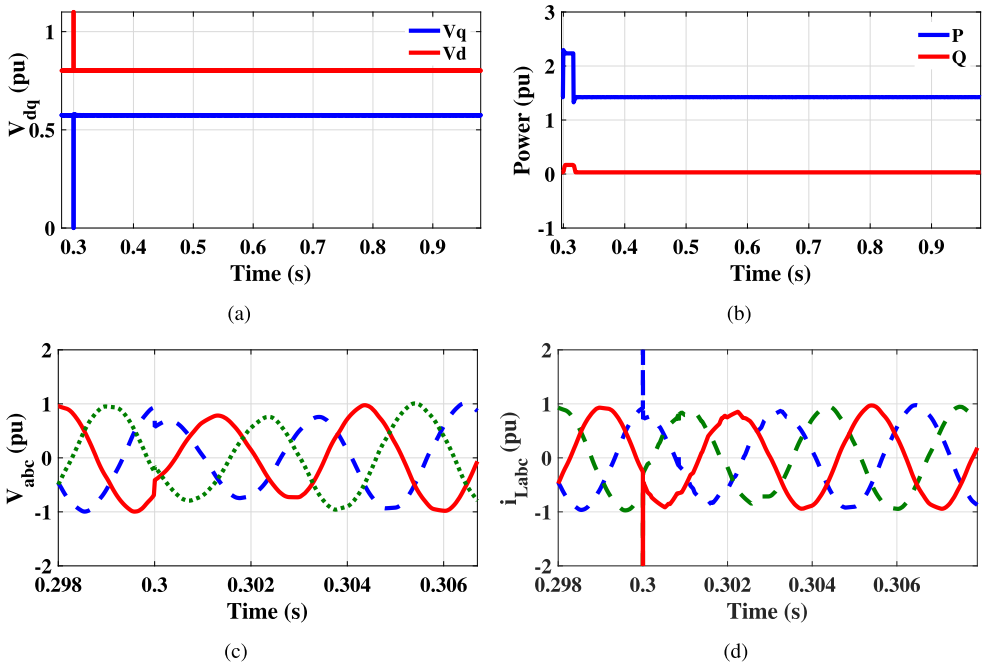

FIGURE 8. Simulation results of the proposed controller against unknown load: (a) d and q components of the load voltage, (b) power components, (c) instantaneous load voltages and their magnitude (solid red (–) line phase a, dashed blue (––) line phase b, and doted green (..) line phase c), (d) instantaneous load currents and their magnitude (solid red (–) line phase a, dashed blue (––) line phase b, and doted green (..) line phase c).

TABLE 2. Comparison of error voltage (RMS value) between the proposed controller, LQR, and LQG controller.

Name of controller	Error voltage for consumer load (V)	Error voltage for harmonic load (V)	Error voltage for asynchronous machine load (V)	Error voltage for dynamic load (V)
Proposed controller	2.50	3.10	5.35	2.20
LQR controller [37]	20.2	21.1	73.8	22.1
LQG controller [37]	10.1	10.3	16.2	12.5

the proposed controller can provide high performance for the three-phase MG. Fig. 7(a) depicts the tracking performance of the reference signals. The power components, voltage and current of MG system are represented in Fig. 7(b), 7(c) and 7(d), respectively. From the results, it is verified that the H_∞ controller is able to regulate the voltage, current and power in a nominal range of three-phase MG.

1) PERFORMANCE UNDER UNKNOWN LOAD

The unknown load circuit in Fig. 6(a) which is used in each phase of the three-phase MG for the consideration of unknown load test. One terminal of the circuit is attached to a single phase while the other terminal is linked to ground. For the closing of switch after t = 0.3s, the load voltage is changed due to the inclusion of unknown load. The MG reference voltages are set to $V_{d,ref}$ and $V_{q,ref}$. After functioning the switch, the load parameter values of the MG system will be changed and is responsible for the change of instantaneous voltage of the system. The dq and power components of load voltage are shown in Fig. 8(a) and 8(b), respectively. Fig. 8(c) and 8(d) show instantaneous load voltages, currents and their magnitude of the MG system against unknown load. The results ensure that the controller achieves desirable performance against the unknown load.

2) PERFORMANCE ANALYSIS OF THREE PHASE NON-LINEAR LOAD

This test shows the performance of the H_∞ controller against a non-linear load. Fig. 6(c) shows a three-phase non-linear load. The nonlinear load for both the single and three phase MG is similar except the bridge rectifier. The load is modeled by a six-pulse diode bridge rectifier. It is linked to the pcc at t = 0.54s and the dq reference signals remain same as before. Fig. 9(a) and 9(b) are the dq and power components, respectively. Fig. 9(c) and 9(d) show the performance of the introduced controller against non-linear load. The results indicate that the controller can keep the voltage and current oscillation in an acceptable range.

C. COMPARATIVE PERFORMANCE ANALYSIS AMONG DIFFERENT CONTROLLERS

The comparative study between the proposed controller, linear quadratic regulator, and the linear quadratic gaussian controller in terms of consumer load, harmonic load,

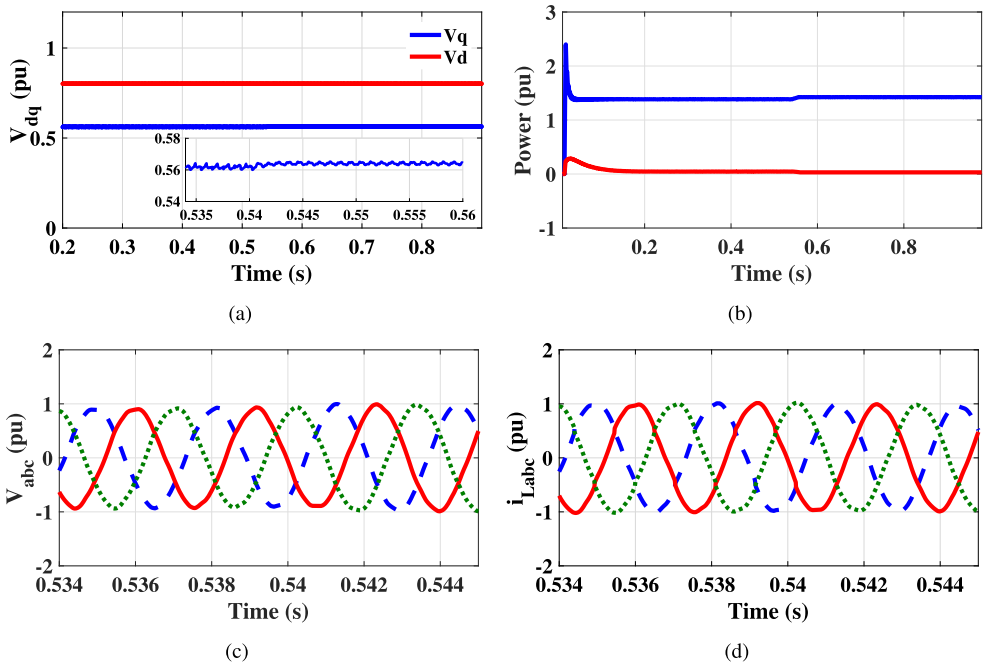

FIGURE 9. Simulation results of the proposed controller against nonlinear load: (a) d and q components of the load voltage, (b) power components, (c) instantaneous load voltages and their magnitude (solid red (–) line phase a, dashed blue (––) line phase b, and doted green (..) line phase c), (d) instantaneous load currents and their magnitude (solid red (–) line phase a, dashed blue (––) line phase b, and doted green (..) line phase c).

TABLE 3. Comparisons of advantages between the controllers.

Name of the controller	Advantages	Limitations
H_∞ Controller	(i) High band width, (ii) Large gain and phase margin, (iii) Robust, (iv) Tracks reference signal	-
LQR Controller	(i) High band width,	(i) cannot follow reference signal, (ii) Low operating region
LQG Controller	(i) High band width,	(i) cannot follow reference signal (ii) Low robustness
Model Predictive Controller	(i) Large gain and phase margin, (ii) Robust, (iii) Low noise	(i) Low band-width

asynchronous machine load and dynamic load is shown in Fig. 4. The results show that the H_∞ controller has better tracking performance than LQR, and LQG controller. The quantitative measurement shown in Table 2 which indicates that the proposed controller has less tracking error with respect to different load conditions. The advantages of the proposed controller compared to other existing controllers available in literature are presented in Table 3. The comparison depicts that the proposed controller ensures high performance as compared to other controllers.

D. ROBUSTNESS ANALYSIS

In this paper, the design of the controller is carried out in a way that the design guarantees the stability of the feedback system against perturbation of plant models. The perturbation of the plant parameters may possibly take place in the form of variation of line impedance and capacitance of the load and so forth. In order to justify the robustness of the proposed controller, a model parameter e.g. capacitor values have been intentionally varied and the performance of the controller against such variation is being tested and measured as shown in the Fig. 10. The results show that the controller provides extensive performance against the variation of capacitor values by tracking the command voltages for islanded operation of the MG. The load of the MG continues changing with respect to time and it is important to guarantee the stability and maintain the voltage, current and power level to a desired level. The designed controller is obliged to perform satisfactorily to a change at the load end. The controller designed in this paper pledges adequate performance for a variation of loads as given in Fig. 4.

Determining the effects of the parameters for this particular type of controller on the obtained results is unrealistic because the controller is designed LMI control problems are usually solved in terms of auxiliary synthesis variables. These variables are connected to the controller parameters through change-of-variables. Typically, constraints are imposed on the auxiliary synthesis variables so as to achieve the desired controller structure. So changing the controller parameters

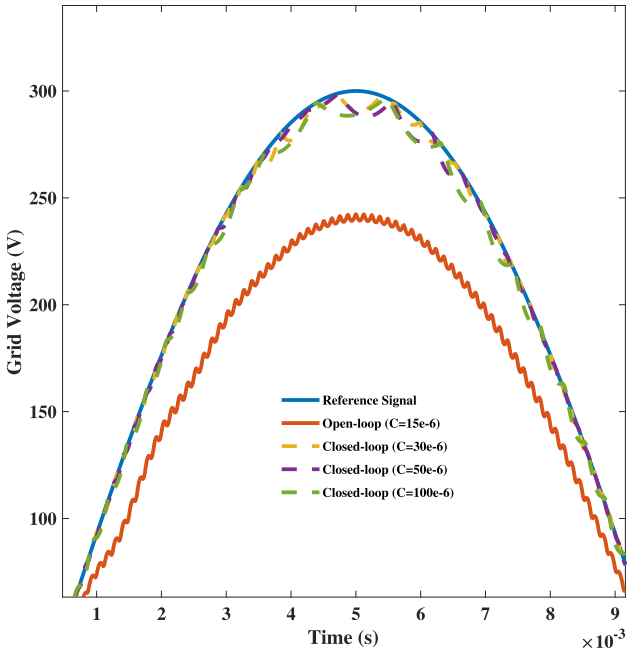

FIGURE 10. Robustness analysis of the proposed controller.

may not led to the feasibility solution of the LMIs and may result in instability.

V. CONCLUSION

This paper presents the design of a high performance extended H_∞ controller for both single and three phase MG. The controller is designed based on the LMI approach. The performance of the proposed control method is investigated considering several uncertainties: unknown load, harmonics load, and non-linear load. The simulation results show that the controller ensures robust performance against uncertainties. The practical implementation and the application of multi-energy source are the future scope of the current research which can be extended for future research.

APPENDIX.

Feasibility of the LMIs is presented in this section. Consider a LTI system

$$\begin{aligned} \dot{x} &= Ax + Bu \\ y &= Cx + Du \end{aligned} \tag{46}$$

where all the state vector $x \in R^n$ and all other vectors and matrices have appropriate dimensions. Using the Lyapunov stability theorem, the system (46) is asymptotically stable if, and only if, there exist a symmetric matrix $L = L^T \in R^{nxn}$ such that the LMI

$$\begin{bmatrix} L & AL \\ LA^T & L \end{bmatrix} > 0 \tag{47}$$

is feasible.

In the above LMI, an instrumental variable is added [39]. It has been shown that system (46) is asymptotically stable if, and only if, there exist a symmetric matrix $L = L^T \in R^{nxn}$ and a general matrix $M = M^T \in R^{nxn}$ such that the LMI

$$\begin{bmatrix} L & AM \\ MA^T & M + M^T - L \end{bmatrix} > 0 \tag{48}$$

is feasible [39].

Now, from the extended H_∞ norm, the inequality $|H_{wz}(s)|_\infty^2 < \eta$ holds stable if, and only if, there exist a symmetric matrix L such that the LMI

$$\begin{bmatrix} L & AL & B & 0 \\ LA^T & L & 0 & LC^T \\ B^T & 0 & I & D^T \\ 0 & CL & D & \eta I \end{bmatrix} > 0 \tag{49}$$

is feasible.

$$\begin{bmatrix} L & AM & B & 0 \\ MA^T & M^T + M - L & 0 & M^T C^T \\ B^T & 0 & I & D^T \\ 0 & CM & D & \eta I \end{bmatrix} > 0 \tag{50}$$

is feasible.

For the proof, choose $M = M^T = L$. Assume that the inequality (50) is feasible. Hence, $M = M^T > L > 0$. It implies that M is non-singular. Since, L is positive definite, the inequality $(L - M)^T L^{-1}(L - M) \geq 0$ holds. Therefore, establishing $ML^{-1}M \geq M^T + M - L$ which yields

$$\begin{bmatrix} L & AM & B & 0 \\ MA^T & M^T + M - L & 0 & M^T C^T \\ B^T & 0 & I & D^T \\ 0 & CM & D & \eta I \end{bmatrix} > 0$$

Which recovers (49) if multiplied on the right by $T = diag[I, M^{-1}L, I, I]$ and on the left by T^T. Now, using the change of variables in (50) as $L = L, M = Y, P = K_c Y$, the proposed state-feedback controller is constructed in a way that there exist symmetric matrix P and other matrices Y and L such that H_∞ norm $|H_{wq}(s)|_\infty^2 < \eta$ satisfies the following LMI.

$$\begin{bmatrix} L & A_{op}Y + B_{12}P & B_{11} & 0 \\ * & Y^T + Y - L & 0 & Y^T C^T + P^T D_{12}^T \\ * & 0 & I & D_{12}^T \\ * & CM & D & \eta I \end{bmatrix} > 0 \tag{51}$$

Solving the above LMI we have found P as

$$P = 10^8 \begin{bmatrix} 3.6 & 0 & 0 & 0.11 \\ 0 & 3.6 & -0.11 & 0 \\ 0 & -0.11 & 0.0036 & 0 \\ 0.11 & 0 & 0 & 0.0036 \end{bmatrix} > 0$$

Which indicates that above LMI (51) is feasible.

REFERENCES

[1] D. Moskovitz, "Profits and progress through distributed resources," Regulatory Assistance Project, Gardiner, ME, USA, Tech. Rep., Feb. 2000.
[2] M. S. Mahmoud, S. A. Hussain, and M. A. Abido, "Modeling and control of microgrid: An overview," *J. Franklin Inst.*, vol. 351, no. 5, pp. 2822–2859, May 2014.
[3] G. Pepermans, J. Driesen, D. Haeseldonckx, R. Belmans, and W. D'haeseleer, "Distributed generation: Definition, benefits and issues," *Energy Policy*, vol. 33, no. 6, pp. 787–798, Apr. 2005.

[4] Z. Zou, Z. Wang, and M. Cheng, "Modeling, analysis, and design of multifunction grid-interfaced inverters with output LCL filter," *IEEE Trans. Power Electron.*, vol. 29, no. 7, pp. 3830–3839, Jul. 2014.

[5] N. W. A. Lidula and A. D. Rajapakse, "Microgrids research: A review of experimental microgrids and test systems," *Renew. Sustain. Energy Rev.*, vol. 15, no. 1, pp. 186–202, Jan. 2011.

[6] R. H. Lasseter, A. A. Akhil, C. Marnay, J. Stephens, J. E. Dagle, R. T. Guttromson, A. S. Meliopoulous, R. J. Yinger, and J. H. Eto, "Integration of distributed energy resources: The CERTS MicroGrid ConceptCERTS," in *Proc. CERTS*, 2003, p. 32.

[7] J. W. Simpson-Porco, F. Dörfler, and F. Bullo, "Voltage stabilization in microgrids via quadratic droop control," *IEEE Trans. Autom. Control*, vol. 62, no. 3, pp. 1239–1253, Mar. 2017.

[8] H. Jiayi, J. Chuanwen, and X. Rong, "A review on distributed energy resources and MicroGrid," *Renew. Sustain. Energy Rev.*, vol. 12, no. 9, pp. 2472–2483, Dec. 2008.

[9] J. A. P. Lopes, C. L. Moreira, and A. G. Madureira, "Defining control strategies for MicroGrids islanded operation," *IEEE Trans. Power Syst.*, vol. 21, no. 2, pp. 916–924, May 2006.

[10] R. Bayindir, E. Hossain, E. Kabalci, and R. Perez, "A comprehensive study on microgrid technology," *Int. J. Renew. Energy Res.*, vol. 4, no. 4, pp. 1094–1107, 2014.

[11] J. M. Guerrero, J. Matas, L. G. De Vicunagarcia De Vicuna, M. Castilla, and J. Miret, "Wireless-control strategy for parallel operation of distributed-generation inverters," *IEEE Trans. Ind. Electron.*, vol. 53, no. 5, pp. 1461–1470, Oct. 2006.

[12] T. C. Green and M. Prodanović, "Control of inverter-based micro-grids," *Electr. Power Syst. Res.*, vol. 77, no. 9, pp. 1204–1213, Jul. 2007.

[13] F. Katiraei, R. Iravani, N. Hatziargyriou, and A. Dimeas, "Microgrids management," *IEEE Power Energy Mag.*, vol. 6, no. 3, pp. 54–65, May/Jun. 2008.

[14] P. L. Villenueve, "Concerns generated by islanding [electric power generation]," *IEEE Power Energy Mag.*, vol. 2, no. 3, pp. 49–53, Jun. 2004.

[15] A. M. Bouzid, J. M. Guerrero, A. Cheriti, M. Bouhamida, P. Sicard, and M. Benghanem, "A survey on control of electric power distributed generation systems for microgrid applications," *Renew. Sustain. Energy Rev.*, vol. 44, pp. 751–766, Apr. 2015.

[16] M.-T. Ho and C.-Y. Lin, "PID controller design for robust performance," *IEEE Trans. Autom. Control*, vol. 48, no. 8, pp. 1404–1409, Aug. 2003.

[17] M. Liserre, R. Teodorescu, and F. Blaabjerg, "Multiple harmonics control for three-phase grid converter systems with the use of PI-RES current controller in a rotating frame," *IEEE Trans. Power Electron.*, vol. 21, no. 3, pp. 836–841, May 2006.

[18] M. Hojabri, A. Z. Ahmad, A. Toudeshki, and M. Soheilirad, "An overview on current control techniques for grid connected renewable energy systems," in *Proc. 2nd Int. Conf. Power Energy Syst. (ICPES)*, Singapore, 2012, pp. 119–126.

[19] M. P. Kazmierkowski and L. Malesani, "Current control techniques for three-phase voltage-source PWM converters: A survey," *IEEE Trans. Ind. Electron.*, vol. 45, no. 5, pp. 691–703, Oct. 1998.

[20] T. Midtsund, "Control of power electronic converters in distributed power generation systems (evaluation of current control structures for voltage source converters operating under weak grid conditions)," M.S. thesis, Dept. Electr. Power Eng., Norwegian Univ. Sci. Technol., Trondheim, Norway, 2010.

[21] A. Timbus, "Grid monitoring and advanced control of distributed power generation systems," Ph.D. dissertation, Inst. Energy Technol., Fac. Eng., Sci. Med., Aalborg Univ., Aalborg, Denmark, May 2007.

[22] Y. A.-R. I. Mohamed and E. F. El-Saadany, "An improved deadbeat current control scheme with a novel adaptive self-tuning load model for a three-phase PWM voltage-source inverter," *IEEE Trans. Ind. Electron.*, vol. 54, no. 2, pp. 747–759, Apr. 2007.

[23] M. C. Chandorkar, D. M. Divan, and R. Adapa, "Control of parallel connected inverters in standalone AC supply systems," *IEEE Trans. Ind. Appl.*, vol. 29, no. 1, pp. 136–143, Jan./Feb. 1993.

[24] F. Katiraei and M. R. Iravani, "Power management strategies for a microgrid with multiple distributed generation units," *IEEE Trans. Power Syst.*, vol. 21, no. 4, pp. 1821–1831, Nov. 2006.

[25] J. M. Guerrero, L. G. de Vicuna, J. Matas, M. Castilla, and J. Miret, "A wireless controller to enhance dynamic performance of parallel inverters in distributed generation systems," *IEEE Trans. Power Electron.*, vol. 19, no. 5, pp. 1205–1213, Sep. 2004.

[26] S. J. Chiang, C. Y. Yen, and K. T. Chang, "A multimodule parallelable series-connected PWM voltage regulator," *IEEE Trans. Ind. Electron.*, vol. 48, no. 3, pp. 506–516, Jun. 2001.

[27] H.-S. Heo, G.-H. Choe, and H.-S. Mok, "Robust predictive current control of a grid-connected inverter with harmonics compensation," in *Proc. 28th Annu. IEEE Appl. Power Electron. Conf. Expo. (APEC)*, Mar. 2013, pp. 2212–2217.

[28] J. M. Espi, J. Castello, R. García-Gil, G. Garcera, and E. Figueres, "An adaptive robust predictive current control for three-phase grid-connected inverters," *IEEE Trans. Ind. Electron.*, vol. 58, no. 8, pp. 3537–3546, Aug. 2011.

[29] A. Sheela, S. Vijayachitra, and S. Revathi, "H-infinity controller for frequency and voltage regulation in grid-connected and islanded microgrid," *IEEJ Trans. Electr. Electron. Eng.*, vol. 10, no. 5, pp. 503–511, Sep. 2015.

[30] H. Bevrani, M. Feizei, and S. Ataee, "Robust frequency control in islanded microgrid: H_∞ and μ-synthesis approaches," *IEEE Trans. Smart Grid*, vol. 7, no. 2, pp. 311–320, 2016.

[31] T. Hornik and Q.-C. Zhong, "A current-control strategy for voltage-source inverters in microgrids based on H^∞ and repetitive control," *IEEE Trans. Power Electron.*, vol. 26, no. 3, pp. 943–952, Mar. 2011.

[32] X. Shen, H. Wang, J. Li, Q. Su, and L. Gao, "Distributed secondary voltage control of islanded microgrids based on RBF-neural-network sliding-mode technique," *IEEE Access*, vol. 7, pp. 65616–65623, 2019.

[33] Y. Shan, J. Hu, M. Liu, J. Zhu, and J. M. Guerrero, "Model predictive voltage and power control of islanded PV-battery microgrids with washout-filter-based power sharing strategy," *IEEE Trans. Power Electron.*, vol. 35, no. 2, pp. 1227–1238, Feb. 2020.

[34] X. Wu, C. Shen, and R. Iravani, "A distributed, cooperative frequency and voltage control for microgrids," *IEEE Trans. Smart Grid*, vol. 9, no. 4, pp. 2764–2776, Jul. 2018.

[35] M. Armin, P. N. Roy, S. K. Sarkar, and S. K. Das, "LMI-based robust PID controller design for voltage control of islanded microgrid," *Asian J. Control*, vol. 20, no. 5, pp. 2014–2025, Sep. 2018.

[36] S. K. Sarkar, M. H. K. Roni, D. Datta, S. K. Das, and H. R. Pota, "Improved design of high-performance controller for voltage control of islanded microgrid," *IEEE Syst. J.*, vol. 13, no. 2, pp. 1786–1795, Jun. 2019.

[37] M. S. Munsi, A. B. Siddique, S. K. Das, S. K. Paul, M. R. Islam, and M. A. Moni, "A novel blended state estimated adaptive controller for voltage and current control of microgrid against unknown noise," *IEEE Access*, vol. 7, pp. 161975–161995, 2019.

[38] M. C. De Oliveira, J. C. Geromel, and J. Bernussou, "Extended H_2 and H_∞ norm characterizations and controller parametrizations for discrete-time systems," *Int. J. Control*, vol. 75, no. 9, pp. 666–679, Jan. 2002.

[39] M. C. de Oliveira, J. Bernussou, and J. C. Geromel, "A new discrete-time robust stability condition," *Syst. Control Lett.*, vol. 37, no. 4, pp. 261–265, Jul. 1999.

MANIZA ARMIN was born in Dhaka, Bangladesh. She received the B.Sc. degree in mechatronics engineering from the Rajshahi University of Engineering & Technology (RUET), Rajshahi, Bangladesh. She is currently working on robust control of smart grid and microgrid. Her research interests include control applications, power system control, IoT, and robotics.

MIZANUR RAHMAN was born in Bangladesh, in 1996. He received the B.Sc. degree in mechatronics engineering from the Rajshahi University of Engineering & Technology (RUET), Rajshahi, Bangladesh. His research interests include control theory and applications, robust control of smart grid, and microgrid. He is also an Active Reviewer of many reputed journals.

MD. MUKIDUR RAHMAN was born in Bangladesh. He received the B.Sc. degree in mechatronics engineering from the Rajshahi University of Engineering & Technology (RUET), Rajshahi, Bangladesh. He is currently working on robust control of smart grid and microgrid. His research interests include control applications, power system control, the IoT, and robotics.

SUBRATA K. SARKER was born in Bangladesh, in 1996. He received the Bachelor of Science degree in mechatronics engineering from the Rajshahi University of Engineering & Technology (RUET), Rajshahi, Bangladesh. He is currently working as a Lecturer with the Department of Electrical and Electronic Engineering, Varendra University, Rajshahi. His research interests include control theory and applications, robust control of electro-mechanical systems, robotics, mechatronics systems, and power system control.

SAJAL K. DAS received the Doctor of Philosophy (Ph.D.) degree in electrical engineering from the University of New South Wales, Australia, in 2014. In May 2014, he was appointed as a Research Engineer with the National University of Singapore (NUS), Singapore. In January 2015, he joined the Department of Electrical and Electronic Engineering, AIUB, as an Assistant Professor. He continued his work at AIUB, until he joined the Department of Mechatronics Engineering, Rajshahi University of Engineering & Technology (RUET), as a Lecturer, in September 2015. He is currently working as an Assistant Professor with RUET. His research interests include control theory and applications, mechatronics system control, robotics, and power system control.

MD. RABIUL ISLAM (Senior Member, IEEE) received the Ph.D. degree in electrical engineering from The University of Technology Sydney (UTS), Sydney, Australia, in 2014. He was appointed as a Lecturer at RUET, in 2005, where he was promoted to a Full Professor, in 2017. In early 2018, he joined the School of Electrical, Computer, and Telecommunications Engineering (SECTE), University of Wollongong (UOW), Wollongong, Australia. He has authored or coauthored 150 articles, including 42 IEEE TRANSACTIONS/IEEE Journal articles, in international journals and conference proceedings. He has written or edited four technical books published by Springer. His research interests include power electronic converters, renewable energy technologies, power quality, electrical machines, electric vehicles, and smart grid. He has received several funding from Government and Industries, including the Australian Government ARC Discovery Project 2020 entitled A Next Generation Smart Solid-State Transformer for Power Grid Applications. He has served as a Guest Editor for the IEEE TRANSACTIONS ON ENERGY CONVERSION, the IEEE TRANSACTIONS ON APPLIED SUPERCONDUCTIVITY, and *IET Electric Power Applications*. He has been serving as an Editor for the IEEE TRANSACTIONS ON ENERGY CONVERSION and the IEEE POWER ENGINEERING LETTERS, and an Associate Editor for IEEE ACCESS.

ABBAS Z. KOUZANI received the B.Sc. degree in computer engineering from the Sharif University of Technology, Iran, the M.Eng.Sc. degree in electrical and electronic engineering from The University of Adelaide, Australia, and the Ph.D. degree in electrical and electronic engineering from Flinders University, Australia. He was a Lecturer with the School of Engineering, Deakin University, Australia, and a Senior Lecturer with the School of Electrical Engineering and Computer Science, The University of Newcastle, Australia. He is currently a Professor with the School of Engineering, Deakin University. He is also the Director of the Deakin University's Advanced Integrated Microsystems (AIM) Research Group. He provides research leadership in embedded, connected, and low-power devices, circuits, and instruments that incorporate sensing, actuation, control, wireless transmission, networking and the IoT, data acquisition/storage/analysis, AI, energy harvesting, power management, and fabrication for tackling research questions relating to a variety of disciplines, including healthcare, ecology, mining, infrastructure, automotive, manufacturing, energy, utilities, and agriculture. He has produced over 370 publications, including one book, 17 book chapters, 180 journal articles, and 181 fully refereed conference papers. He has three patents and two pending patents. He has been involved in over 15 million research grants, and has managed projects and delivered research solutions to over 25 Australian and International companies. He has supervised 24 research fellows/assistants, and produced 28 Ph.D. and six Masters by Research completions. He is also involved in supervision of 12 Ph.D. students. He received several awards, including the Outstanding Contribution to Scholarly Publication Award from the School of Engineering, Deakin University, in 2019.

M. A. PARVEZ MAHMUD received the B.Sc. degree in electrical and electronic engineering and the Master of Engineering degree in mechatronics engineering. After the successful completion of his Ph.D. degree with multiple awards, he has worked as a Postdoctoral Research Associate and an Academician with the School of Engineering, Macquarie University, Sydney. He has worked as a Lecturer with the World University of Bangladesh (WUB), for more than two years, and a Researcher with the Korea Institute of Machinery and Materials (KIMM), for about three years. He is currently an Alfred Deakin Postdoctoral Research Fellow with Deakin University. His research interests include energy sustainability/harvesting, sensors, and electric microgrid control and management.